Electronic Supplementary Material (ESI) for Nanoscale.

Nanoscale

Supporting Information

Efficient Plasma-enhanced Method of Layered $LiNi_{1/3}Co_{1/3}Mn_{1/3}O_2$ cathodes with Sulfur Atom-scale Modification for Superior-Performance Li-ion Batteries

Qianqian Jiang[a,b], Ning Chen[b], Dongdong Liu[b], Shuangyin Wang[b,*], Han Zhang[a,*]

[a] SZU-NUS Collaborative Innovation Center for Optoelectronic Science and Technology, Key Laboratory of Optoelectronic Devices and Systems of Ministry of Education and Guangdong Province, College of Optoelectronic Engineering, Shenzhen University, Shenzhen, 518060, P. R. China

[b] State Key Laboratory of Chem/Bio-Sensing and Chemometrics, College of Chemistry and Chemical Engineering, Hunan University, 410082, Changsha , P. R. China.

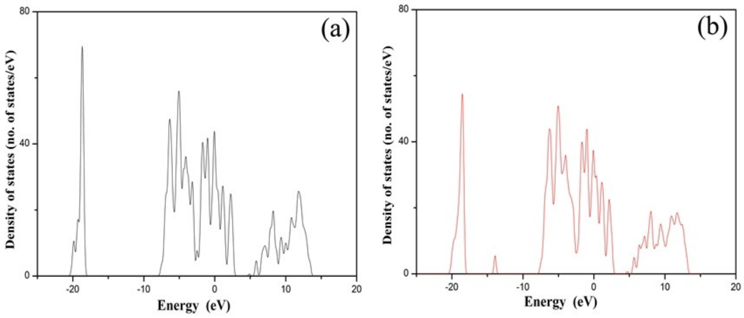

Fig. S1 Density of states (DOS) of LNCM and LNCM-S-20

Table S1 The crystal structures, total energy and binding energy values (E_b) of LNCM and LNCM-S. *not mentioned

Sample	E_b (eV)	α	β	γ	a (Å)	b(Å)	c(Å)
LNCM (Total)	-297.1650	90.0703	89.9699	119.5801	5.7627	5.7221	14.1018
LNCM-S-20 (Total)	-293.6936	90.0842	89.8537	119.2383	5.8208	5.7725	14.3440
O	-0.0002	*	*	*	*	*	*
S	-0.0160	*	*	*	*	*	*

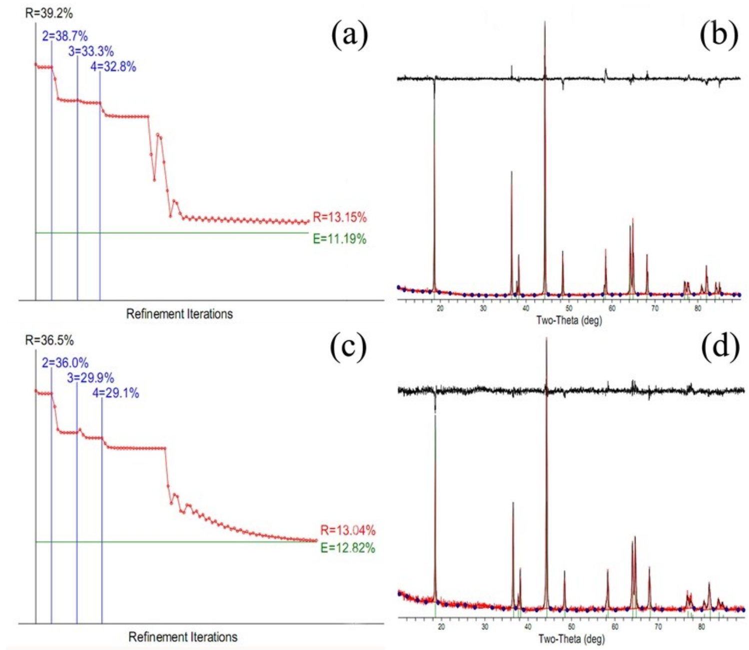

Fig. S2. Refinement parameters and the refined XRD patterns of LNCM (a and b) and LNCM-S-20 (c and d)

Table S2 Lattice parameters of LNCM and LNCM-S-20

Sample	a (Å3)	c (Å3)	c/a	I_{003}/I_{004}
LNCM	2.858	14.230	4.979	1.29
LNCM-S-20	2.854	14.227	4.985	1.28

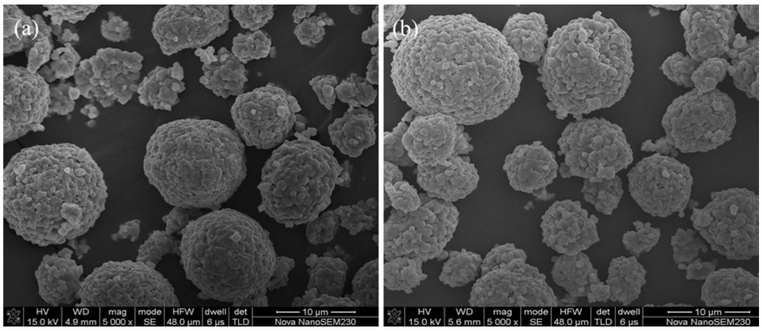

Fig. S3. SEM images of (a) sample LNCM and (b)LNCM-S-20 show highly aggregated particles. Scale bars: 10 μm

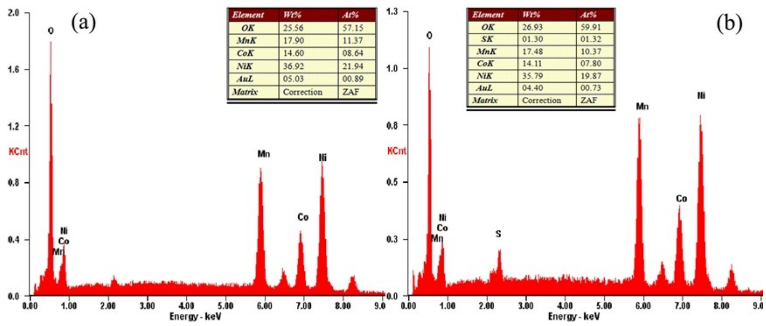

Fig. S4. EDAX results of (a) sample LNCM and (b)LNCM-S-20

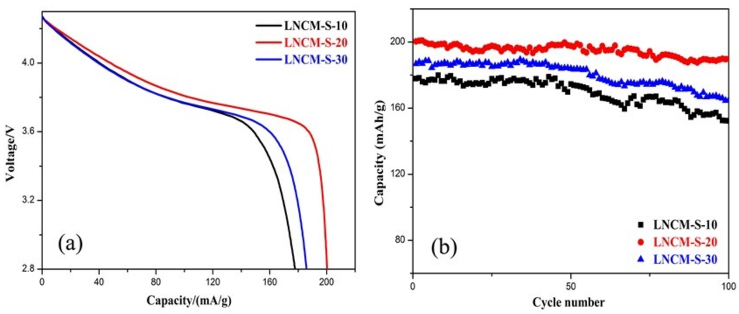

Fig. S5. Initial discharge curves (a) and cycling stability curves (b) of sample with different plasma times

The initial discharge curves of of sample with different plasma times at the rates of 0.2 C are shown in Fig.S5. All the discharge curves exhibit one obvious discharge plateaus associated with the one-stage mechanism of the electrochemical lithium intercalation and extraction at about 3.9 V [1, 2]. From Fig. S5a, it can be clearly seen that LNCM-S-20 has the largest initial discharge (200.4 mAh·g^{-1})of the three samples, which indicates the reaction time of 20 min is the optimal plasma time to synthesize $LiNi_{1/3}Co_{1/3}Mn_{1/3}O_{2-x}S_x$ with the excellent electrochemical performance. Though the initial discharge of PLA-LNCM-S-10 and PLA-LNCM-S-30 are 177.8 mAh·g^{-1} and 185.9 mAh·g^{-1}, which is small than that of LNCM-S-20, this result is much higher than that of the pristine $LiNi_{1/3}Co_{1/3}Mn_{1/3}O_2$, which indicates the S doping is good for the electrochemical performance.

Fig. S5b shows the cycle performance of samples with different plasma times. In particular, when the plasma time is 20 min, good discharge capacity and excellent cycle performance are obtained. The first discharge capacity is 200.4 mAh·g^{-1}, and the capacity was 189.7 mAh·g^{-1} after 100 cycles, retaining 94.46% of the original values. However, the PLA-LNCM-S-10 and PLA-LNCM-S-30 can only contain 85.60% and 8.12% after 100 cycles of their initial discharge capacities, which is lower than that of LNCM-S-20, which further confirms the optimal plasma time is 20 min. Therefore, These data illustrate that sample with the plasma time of 20 min shows best electrochemical properties because of moderate crystallinity.

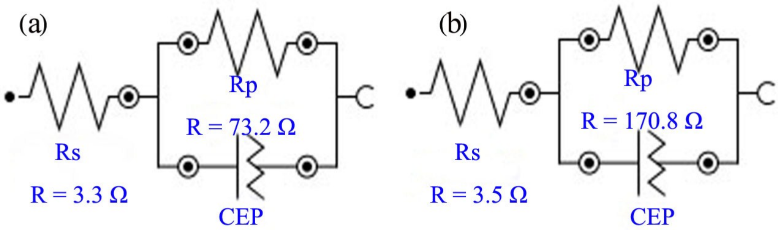

Fig. S6. Electrochemical impedance spectroscopy (EIS) fitting results for a) pristine LNCM and b) LNCM-S-20. Rs: electrolyte resistance, Rp: charge-transfer resistance, CPE: constant-phase element.

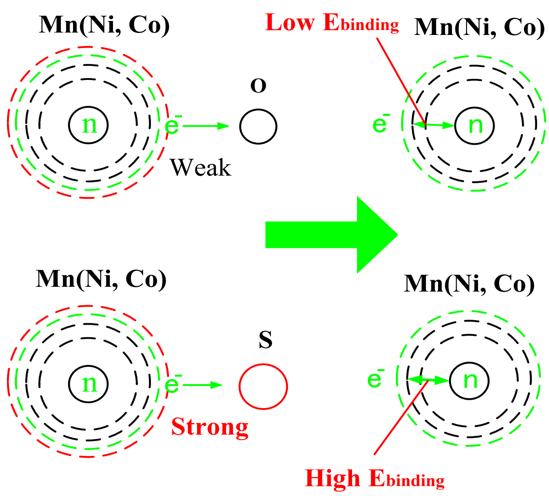

Fig. S7. The scheme to illustrate the X-ray photoelectron spectroscopy for Mn (Ni, Co) 2p core peak shift by the doping of S.

Table S3. Representative electrochemical performance for $LiNi_{1/3}Co_{1/3}Mn_{1/3}O_2$ modified with different method from literature. *not mentioned

Method	Modification Method	Initial Discharge (mAh/g)	Cut off condition（V）	Capacity retention (%)
Plasma-enhanced Method(This work)	Sulfur Atom-scale Modification	200.4	2.8-4.3	94.46%
Solid State Reaction with V_2O_5[3]	Li_3VO_4-coated on the surface	198.2	3.0 – 4.6	87.5%
Solid State Reaction with Nb_2O_5[4]	Zn substitution on the crystal structure	162.9	2.8 - 4.4	95.1 (50 cycles)
Solid State Reaction with $LiOH·H_2O$ and H_3BO_3[5]	coated by lithium boron oxide on the surface	185.1	2.5 - 4.5	93.4 (50 cycles)
Solid State Reaction with $Zr(OC_4H_9)_4$[6]	Coated Li_2ZrO_3 on the surface	192	3.0 - 4.5	*
Solid State Reaction with $Zr(OC_4H_9)_4$ and $CH_3COOLi·2H_2O$[7]	Coated Li_2ZrO_3 on the surface	178.1	2.5 - 4.4	92
Solid State Reaction with $Zr(OC_4H_9)_4$[8]	Li_2ZrO_3-coated on the surface	200.4	3.0 - 4.6	89
Solid State Reaction with LiF[9]	Fluorine substitution on the crystal structure	about 171	2.8 - 4.6	About 93 (50 cycles)
Solid State Reaction with LiF[10]	LiF modification on the surface	168.1	2.5 - 4.5	92.8

Reference

1. N. Yabuuchi and T. Ohzuku, *J. Power Sources*, 2003, **119**, 171.

2. K. Shaju, G. S. Rao and B. Chowdari, *Electrochim. Acta*, 2002, **48**, 145.

3. W. Wang, Z. Yin, Z. Wang, X. Li and H. Guo, *Mater. Lett.*, 2015, **160**, 298.

4. H. Du, Y. Zheng, Z. Dou and H. Zhan, *Journal of Nanomaterials*, 2015, **2015**, 1.

5. S. Y. Tan, L. Wang, B. Liang, J. B. Xu, W. Ren, P. F. Hu and A. M. Chang, *J. Power Sources*, 2014, **277**, 139.

6. J. Zhang, Z. Li, R. Gao, Z. Hu and X. Liu, *The Journal of Physical Chemistry C*, 2015, **119**, 20350.

7. C. Wang, L. Chen, H. Zhang, Y. Yang and F. Wang, *Electrochim. Acta*, 2013, **119**, 236.

8. W. Wang, Z. Yin, Z. Wang, X. Li and H. Guo, *Journal of Alloys & Compounds*, 2015, **651**, 737.

9. G. H. Kim, M. H. Kim, S. T. Myung and K. S. Yang, *J. Power Sources*, 2005, **146**, 602.

10. S. J. Shi, J. P. Tu, Y. Y. Tang, Y. Q. Zhang, X. Y. Liu, X. L. Wang and C. D. Gu, *J. Power Sources*, 2013, **225**, 338.